

## Article

# Degenerated Boundary Layers and Long-Wave Low-Frequency Motion in High-Contrast Elastic Laminates

Lenser A. Aghalovyan <sup>1,†</sup>, Lusine G. Ghulghazaryan <sup>1,2,†</sup>, Julius Kaplunov <sup>3,\*,†</sup>  and Danila Prikazchikov <sup>3,†</sup>

<sup>1</sup> Institute of Mechanics, National Academy of Sciences of the Republic of Armenia, Yerevan 0019, Armenia; lagal@sci.am (L.A.A.); lusina@mail.ru (L.G.G.)

<sup>2</sup> Faculty of Mathematics, Physics and Informatics, Department of Mathematics and its Teaching Methods, Armenian State Pedagogical University after Khachatur Abovyan, Abovyan 0010, Armenia

<sup>3</sup> School of Computer Science and Mathematics, Keele University, Keele, Staffordshire ST5 5BG, UK; d.prikazchikov@keele.ac.uk

\* Correspondence: j.kaplunov@keele.ac.uk

† These authors contributed equally to this work.

**Abstract:** The effect of high contrast on the multiscale behaviour of elastic laminates is studied. Mathematical modelling in this area is of significant interest for a variety of modern applications, including but not limited to advanced sandwich structures and photovoltaic panels. As an example, the antiplane shear of a symmetric, three-layered plate is considered. The problem parameters expressing relative thickness, stiffness and density are assumed to be independent. The high contrast may generally support extra length and time scales corresponding to degenerated boundary layers and propagating long-wave low-frequency vibration modes. The main focus is on the relation between these two phenomena. The developed multiparametric approach demonstrates that those do not always appear simultaneously. The associated explicit estimates on contrast parameters are established. In addition, the recent asymptotic extension of the classical Saint-Venant's principle is adapted for calculating the contribution of the degenerate boundary layer or long-wave low-frequency propagation mode. The peculiarity of the limiting absorption principle in application to layered media is also addressed.

**Keywords:** laminate; high contrast; multiparametric; multiscale; asymptotic; Saint-Venant's principle; boundary layer; long-wave; low-frequency; radiation conditions

**MSC:** 74J05; 74B05; 74G50



**Citation:** Aghalovyan, L.A.; Ghulghazaryan, L.G.; Kaplunov, J.; Prikazchikov, D. Degenerated Boundary Layers and Long-Wave Low-Frequency Motion in High-Contrast Elastic Laminates. *Mathematics* **2023**, *11*, 3905. <https://doi.org/10.3390/math11183905>

Academic Editor: Hovik Matevosian

Received: 13 August 2023

Revised: 10 September 2023

Accepted: 11 September 2023

Published: 14 September 2023



**Copyright:** © 2023 by the authors. Licensee MDPI, Basel, Switzerland. This article is an open access article distributed under the terms and conditions of the Creative Commons Attribution (CC BY) license (<https://creativecommons.org/licenses/by/4.0/>).

## 1. Introduction

The mathematical modelling of layered elastic structures has been a subject of numerous publications; see, e.g., [1–4] and references therein. More recently, a growing interest in high-contrast laminates has been inspired by modern important applications, including laminated glass, photovoltaic panels, lightweight sandwich-type structures; see, e.g., [5–8]. In addition, we mention the related contributions [9–11].

Two of the most significant observations regarding high-contrast layered structures include a degeneration of the boundary layers, demonstrating slow decay into the interior, studied in [12–15], along with the emergence of a specific low-frequency shear vibration spectra, characterised by a small cut-off frequency with the value tending to zero as powers of small parameters standing for contrast (see [16]) treating three-layered symmetric papers for several mechanical and geometrical setups; see also [17]. The eigenvalue problem on the plate's transverse cross section also arises in the case of free longitudinal vibrations of a strongly inhomogeneous, three-component rod [18]. The presence of an extra low-frequency shear mode supports two-mode long-wave low-frequency asymptotic theories for asymmetric three-layered strips, subject to antiplane elastic deformation; see [19].

The cited paper also suggests a non-trivial asymptotic generalisation of Saint-Venant's principle for the considered high-contrast scenario, stating the consistent boundary conditions (see also [20]) for extension to the anti-plane shear of multi-layered structures. The extra approximate boundary condition in [19] ensures the equilibrium of stress couples applied along the contour of a soft layer. The number of extra asymptotic boundary conditions in [20] coincides with that of soft layers and may be interpreted in a similar manner.

The relation between the degenerated boundary layers and the extra low-frequency modes has not yet been studied systematically, with the exception of [19], addressing only one specific parametric setup. At the same time, the static analysis in [12–14] is mainly restricted to studying the roots of the related transcendental equation without a more general insight into the peculiarities of the stress and strain fields. The main objective of the present paper is elucidation of the link between these two phenomena. Enhanced understanding of this link is relevant for new technological advances over virtually all of the above-mentioned applications, including modern sandwich panels.

A basic example of the antiplane problem in dynamic elasticity for a three-layered high-contrast symmetric laminate with Neumann boundary conditions on the faces is considered. The results of the full multiparametric analysis are presented for the anti-symmetric low-frequency wave. In this case, the ratios of thicknesses, stiffnesses and densities of the layers are assumed to be independent of each other. The tackled example clearly illustrates a multiscale nature of the high contrast effect. Indeed, it brings an extra relatively large length scale (compared to thickness) corresponding to a degenerate boundary layer, as well an extra time scale (small compared to the time elastic waves take to propagate the distance of order thickness) associated with the lowest cut-off, in addition to laminate thickness. Obviously, the aforementioned length and time scales do not arise in non-contrast situations.

It is established that the extra low-frequency modes do not always accompany the degenerate boundary layers. It is shown that both uniform and non-uniform approximations of the associated dispersion curve are possible. The asymptotic bounds on the problem parameters, corresponding to various options are found. Numerical illustrations are presented.

Another emphasis of the paper is on the explicit solution of the forced problem for a semi-infinite symmetric three-layered strip with traction-free faces under a self-equilibrated edge stress. The decay condition in [19] generalising Saint-Venant's principle is adapted. Above the cut-off frequency, this transforms to a radiation condition aimed at excluding the long-wave propagating mode; see [21] for more detail. As a result, the amplitude of the mode of interest is found. In addition, the peculiarity of the implementation of the limiting absorption principle for layered structures is briefly addressed for the long propagating mode originating from the cut-off in question. Along with the analysis of the coexistence of slowly decaying boundary layers and low-frequency vibration modes, this also contributes to the novelty of the paper.

The paper is organised as follows. The problem is formulated in Section 2 with the dispersion relation and the associated eigensolutions derived in Section 3. Section 4 is concerned with multiparametric analysis of the dispersion relation. The main result of the paper addressing the general issue of the relation between the degenerated boundary layer and the low-frequency cut-off is also exposed in this section. The explicit solution to the forced time-harmonic problem for a semi-infinite three-layered strip is obtained in Section 5. Several concluding remarks are summarised in Section 6.

## 2. Problem Statement

Consider a semi-infinite, three-layered, symmetric, elastic laminate; see Figure 1. Let the horizontal axis pass through the middle of the inner layer. Then, the latter occupies the domain  $\{0 \leq x_1 < \infty, -h_1 \leq x_2 \leq h_1, -\infty < x_3 < \infty\}$ , whereas the outer skin layers are located at  $\{0 \leq x_1 < \infty, h_1 \leq |x_2| \leq h_1 + h_2, -\infty < x_3 < \infty\}$ . Below, we focus on antiplane shear motion, with the displacement field given by  $\mathbf{u} = (0, 0, u_3(x_1, x_2, t))$ , more

specifically, on an antisymmetric problem, for which the out-of-plane displacement satisfies  $u_3(x_1, -x_2, t) = -u_3(x_1, x_2, t)$ .

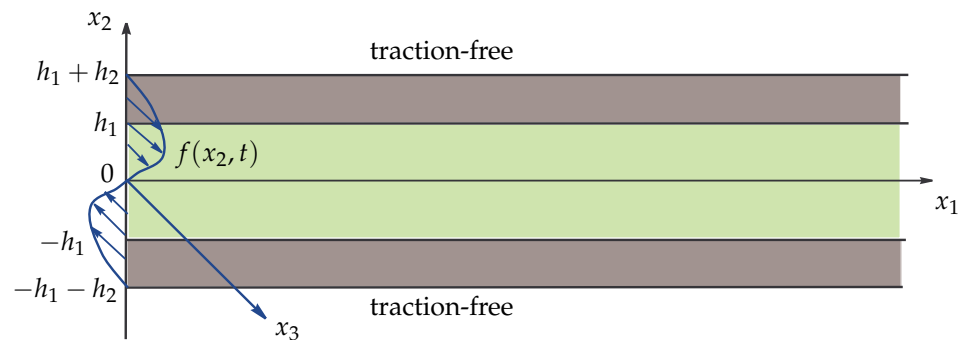


Figure 1. Schematic of a three-layered laminate.

The wave equations of motion are written conventionally as

$$\Delta u_3 - \frac{1}{c^2} \frac{\partial^2 u_3}{\partial t^2} = 0, \tag{1}$$

where  $\Delta = \frac{\partial^2}{\partial x_1^2} + \frac{\partial^2}{\partial x_2^2}$  is the two-dimensional Laplacian in  $x_1$  and  $x_2$ , and the transverse wave speed  $c$  is defined as

$$c = \begin{cases} \sqrt{\frac{\mu_1}{\rho_1}}, & |x_2| \leq h_1; \\ \sqrt{\frac{\mu_2}{\rho_2}}, & h_1 \leq |x_2| \leq h_1 + h_2. \end{cases} \tag{2}$$

Here,  $\mu_i$  and  $\rho_i$  ( $i = 1, 2$ ) stand for the shear moduli and volume mass densities of the core and skin layers, respectively.

The traction-free boundary conditions at the faces  $x_2 = \pm(h_1 + h_2)$  are assumed, i.e.,

$$\sigma_{32} = 0, \tag{3}$$

while the perfect contact conditions along the interfaces  $x_2 = \pm h_1$  are formulated as

$$[u] = 0, \quad [\sigma_{32}] = 0, \tag{4}$$

where  $[\ ]$  indicate jumps of the associated quantities.

Here and below, the stresses  $\sigma_{3j}$  ( $j = 1, 2$ ) are given by

$$\sigma_{3j} = \begin{cases} \mu_1 \frac{\partial u_3}{\partial x_j}, & |x_2| \leq h_1; \\ \mu_2 \frac{\partial u_3}{\partial x_j}, & h_1 \leq |x_2| \leq h_1 + h_2. \end{cases} \tag{5}$$

In addition, let a shear edge loading be modelled by the boundary condition

$$\sigma_{31} = f(x_2, t) \tag{6}$$

at  $x_1 = 0$ , where  $f(x_2, t)$  is a prescribed stress, being an odd function in  $x_2$ , for the sake of simplicity, in order to exclude the fundamental mode from the consideration. At infinity  $x_1 \rightarrow \infty$ , we impose decay or radiation conditions on the sought-for solution.

The formulated problem has a clear multiparametric nature, characterised by several dimensionless parameters, including the relative stiffness, density and thickness, given by

$$\mu = \frac{\mu_1}{\mu_2}, \quad \rho = \frac{\rho_1}{\rho_2}, \quad \text{and} \quad h = \frac{h_1}{h_2}. \tag{7}$$

Below all of them are assumed to be independent unless specified otherwise. The problem apparently provides the simplest step forward from 1D analysis in [18] to a 2D setup.

### 3. Dispersion Relation

First, we introduce the travelling wave ansatz for the displacement in the form

$$u_3 = A(x_2)e^{i(kx_1 - \omega t)}, \tag{8}$$

where  $k$  and  $\omega$  conventionally denote the wave number and angular frequency, respectively, and  $A(x_2)$  is a sought for odd function; hence, below, we may restrict ourselves to the interval  $0 \leq x_2 \leq h_1 + h_2$ .

Then, we infer from (1) that

$$A(x_2) = \begin{cases} A_1 \sin(\alpha_1 \eta), & 0 \leq \eta \leq \frac{h}{h+1}; \\ A_2 \sin(\alpha_2 \eta) + A_3 \cos(\alpha_2 \eta), & \frac{h}{h+1} \leq \eta \leq 1, \end{cases} \tag{9}$$

where

$$\eta = \frac{x_2}{h_1 + h_2} \tag{10}$$

is the dimensionless transverse variable;  $A_1, A_2$  and  $A_3$  are arbitrary real constants; and the parameters  $\alpha_1$  and  $\alpha_2$  are defined by

$$\alpha_1 = \sqrt{(1 + h^{-1})^2 \Omega_1^2 - K^2}, \quad \alpha_2 = \sqrt{(1 + h)^2 \Omega_2^2 - K^2}, \tag{11}$$

with

$$K = k(h_1 + h_2), \quad \text{and} \quad \Omega_j = \omega h_j \sqrt{\frac{\rho_j}{\mu_j}}, \quad j = 1, 2, \tag{12}$$

standing for the dimensionless wave number and frequencies, respectively.

Next, inserting (8) and (9) into boundary and interfacial conditions (3) and (4), we arrive at the dispersion relation

$$\frac{\alpha_2}{\alpha_1} \tan\left(\frac{\alpha_1 h}{1 + h}\right) \tan\left(\frac{\alpha_2}{1 + h}\right) = \mu. \tag{13}$$

The eigenform amplitude  $A(x_2)$  is then given by

$$A(x_2) = \begin{cases} C \cos\left(\frac{\alpha_2}{h+1}\right) \sec(\alpha_2) \csc\left(\frac{\alpha_1 h}{h+1}\right) \sin(\alpha_1 \eta), & 0 \leq \eta \leq \frac{h}{h+1}; \\ C[\tan(\alpha_2) \sin(\alpha_2 \eta) + \cos(\alpha_2 \eta)], & \frac{h}{h+1} \leq \eta \leq 1, \end{cases} \tag{14}$$

where  $C$  is an arbitrary constant.

In what follows, we consider the long-wave low-frequency behaviour of this dispersion relation, assuming that

$$|K| \ll 1 \quad \text{and} \quad \Omega_i \ll 1. \tag{15}$$

This setup has been earlier defined as a global low-frequency one (see [18]), since it is associated with polynomial variation of the sought-for displacement field across the thickness within each of the layers. The absolute value of  $K$  in (15) indicates that both propagating and evanescent modes are studied.

#### 4. Multiparametric Analysis

Below, the dispersion relation (13) is subject to asymptotic analysis in three independent parameters (7) over the long-wave low-frequency domain (15). As mentioned above, the focus is on the relation between the two most importance consequences of high contrast, namely the degeneration of boundary layers and the shift of cut-off frequencies to the low-frequency domain. It is worth noting that the latter are related to specific extra scales, including a large length scale and slow time scale, respectively. For these scales, a typical decaying rate is much greater than the laminate thickness, and a characteristic time considerably exceeds that elastic waves take to propagate the distance between laminate faces.

Consider first the static limit at  $\Omega_i = 0$ . In this case, the transcendental equation has small imaginary roots

$$K = \pm iK_*,$$

where, at leading order,

$$K_* \approx \sqrt{\frac{\mu}{h}}(h + 1) \ll 1, \tag{16}$$

provided that

$$\mu \ll \frac{h}{(h + 1)^2}. \tag{17}$$

In contrast to homogeneous structures, the root  $K_*$  corresponds to the so-called degenerated boundary layer, which does not decay at the distances of order thickness away from the edge. The asymptotic behaviour (16) was earlier established in [12]. However, the two-parametric origin of the problem was not taken into consideration; namely, it was supposed that  $h \sim 1$ . As a result, the restriction (17) has not appeared in the cited paper.

Next, turn to the asymptotic analysis of the lowest cut-off frequencies, coming from the dispersion relation (13) at  $K = 0$ . In this case, the aforementioned global low-frequency regime ( $\Omega_j \ll 1, j = 1, 2$ ) takes place over the following parameter range:

$$\mu \ll h \ll \frac{1}{\rho}, \tag{18}$$

see [16,18] for more detail. Then, for the sought-for cut-off frequency

$$\Omega_2 = \Omega_* \approx \sqrt{\frac{\mu}{h}} \tag{19}$$

or

$$\Omega_1 = \sqrt{\frac{\rho}{\mu}} h \Omega_* \approx \sqrt{\rho h}. \tag{20}$$

It might be easily verified that a non-contrast setup, for which  $\Omega_* \sim 1$ , does not support low-frequency cut-offs.

Let us now investigate the inequalities (17) and (18) simultaneously. First of all, it is clear that for  $h \lesssim 1$ , i.e., excluding the laminates with thin skin, the condition (18)

guarantees not only a low cut-off, but also a slowly decaying static boundary layer. More generally, both phenomena occur when

$$\mu \ll \frac{h}{(h+1)^2} \quad \text{and} \quad h \ll \frac{1}{\rho}. \tag{21}$$

In particular, for  $h \gg 1$ , i.e., for conventional sandwiches with thin skin, the low-frequency vibration mode appears along with the strongly localised static boundary layer (typical of homogeneous or weakly inhomogeneous structures), provided that

$$\frac{1}{h} \ll \mu \ll h \ll \frac{1}{\rho}. \tag{22}$$

Next, by taking leading-order Taylor expansions, we derive a shortened form of the dispersion relation (13). It is given by

$$\alpha_2^2 = \mu \frac{(1+h)^2}{h}, \tag{23}$$

or, equivalently,

$$\Omega_2^2 - \frac{K^2}{(1+h)^2} = \Omega_*^2. \tag{24}$$

As might be expected, the last equation implies the values of  $K = K_*$  at  $\Omega_2 = 0$ , and also  $\Omega_2 = \Omega_*$  at  $K = 0$ , which is in agreement with the estimates (16) and (19), respectively. Moreover, it is obvious that the approximation (24) of the full dispersion relation is uniformly valid over the domain

$$|K| \leq K_*, \quad 0 \leq \Omega_2 \leq \Omega_*, \tag{25}$$

provided that the conditions (17) and (18) are satisfied. The shortened dispersion relation (24) also shows that the quasi-static limit occurs at  $\Omega_2 \ll \Omega_*$ .

At the same time, above the cut-off frequency, the validity range of the approximation (24) is given by

$$K \ll \min \left\{ 1, \frac{1+h}{h} \sqrt{\frac{\mu}{\rho}} \right\} \tag{26}$$

and

$$\Omega_2^2 - \Omega_*^2 \ll \min \left\{ \frac{1}{(1+h)^2}, \frac{\Omega_*^2}{\rho h} \right\}. \tag{27}$$

These strong inequalities generalise earlier considerations for one-parametric setups in [16,19].

Let us now present several graphical illustrations highlighting the observations above. First, we present a sketch characterising the domains corresponding to conditions (17) and (18) in parametric space. For the sake of clarity, we present a 2D graph in  $\mu$  and  $h$  only, but bearing in the mind the restriction  $h \ll \frac{1}{\rho}$ , which is assumed to be valid. The highlighted domains in Figure 2 correspond to various ranges of the dimensionless parameters  $\mu$  and  $h$ , defined by the conditions (17) and (18), for which the latter are either satisfied simultaneously (yellow), or the relation (18) holds but (17) is violated (green), or when both (17) and (18) fail (blue).

Now, let us illustrate the case of a small cut-off frequency along with a rapidly decaying boundary layer, i.e., when the the strong inequalities (18) are satisfied but condition (17) is violated. It is clearly seen from Figure 3, displaying the approximate curve (24) covering both domains of the real and imaginary wavenumber  $K$ . The approximate value in the static limit at  $\Omega_2 = 0$  and  $K \approx 3.5i$  on the approximate curve (24) is far off from the numerical solution of the exact dispersion relation (13) at  $\Omega_2 = 0$ ,  $K_* \approx 1.6i$ . At the same

time, the approximate curve is clearly passing very close to the exact point of the cut-off frequency  $K = 0, \Omega_2 = \Omega_*$ .

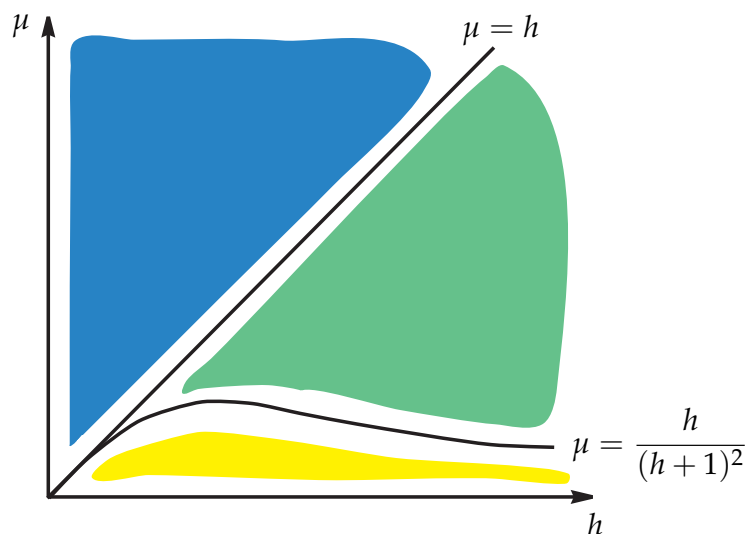


Figure 2. Validity of the strong inequalities (17) and (18) in  $\mu$ - $h$  plane.

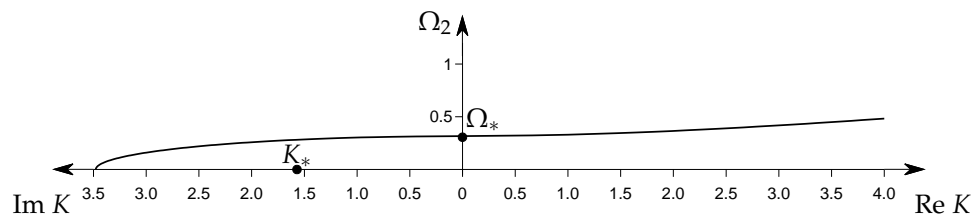


Figure 3. Approximation (24), the exact static limit  $K_*$ , and the lowest cut-off frequency  $\Omega_*$  for the dimensionless parameters (7) chosen as  $\mu = 1, h = 10, \rho = 0.01$ .

An opposite scenario is presented in Figure 4, in which the parameters  $\mu = 0.1, h = 1$  and  $\rho = 10$  are chosen such that the condition (17) is satisfied, and the inequalities (18) do not hold. Consequently, it is observed that the approximate curve (24) passes close to the static limit  $K_*$ , but misses considerably on the cut-off frequency  $\Omega_*$ .

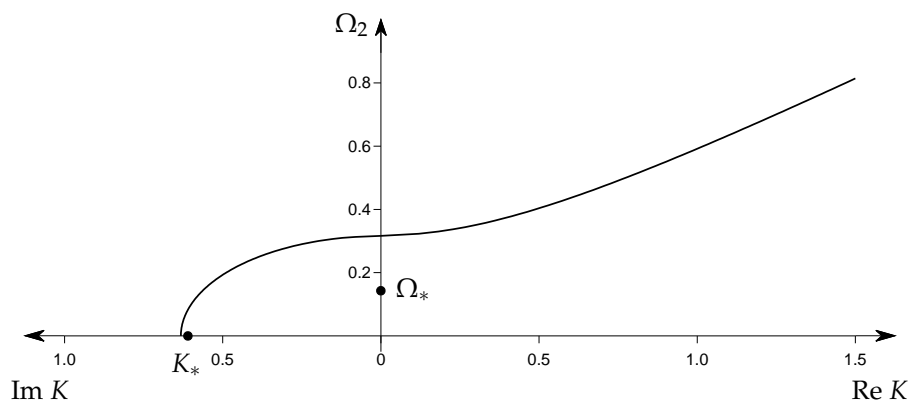


Figure 4. Approximation (24) and the exact static limit  $K_*$  and lowest cut-off frequency  $\Omega_*$  for the dimensionless parameters (7) taken as  $\mu = 0.1, h = 1, \rho = 10$ .

Finally, we are displaying the setup when both conditions (17) and (18) are satisfied; see Figure 5. In this case, the approximate curve (24) is shown by a dashed line and is

complemented by the exact dispersion (13), depicted by solid curve. It is also remarkable that approximation (24) provides a uniform approximation both for decaying and propagating modes.

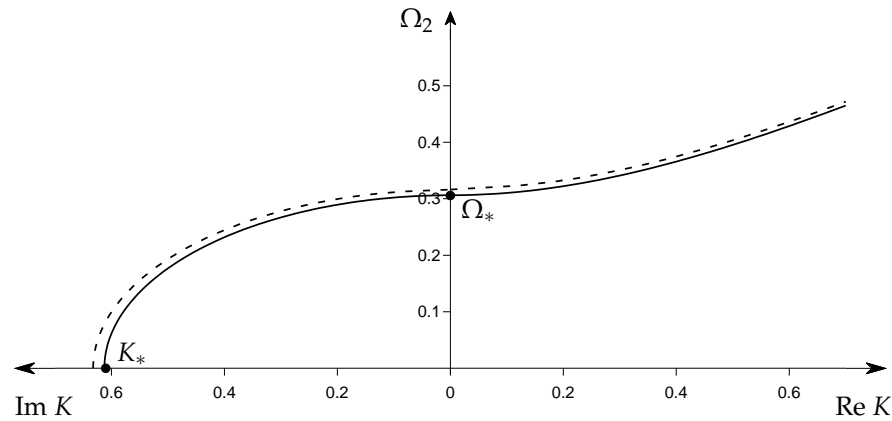


Figure 5. Dispersion curve (13) (solid line) and its approximation (24) (dashed line) for the dimensionless parameters (7) specified as  $\mu = 0.1, h = 1,$  and  $\rho = 0.1$ .

### 5. Forced Vibration

Consider now time-harmonic forced vibration of a semi-infinite laminate, starting from the formulation in Section 2. For the sake of simplicity, restrict ourselves to a one-parametric scenario in which  $\mu \ll 1, h \sim 1$  and  $\rho \sim \mu$ . In this case, as follows from (14), the leading-order behaviour of the eigenform becomes

$$A(x_2) = \begin{cases} C \frac{h+1}{h} \eta, & 0 \leq \eta \leq \frac{h}{h+1}; \\ C, & \frac{h}{h+1} \leq \eta \leq 1. \end{cases} \tag{28}$$

To determine the constant  $C$ , we adapt the decay conditions in [19,20], generalising the classical Saint-Venant’s principle for high-contrast laminates. For a three-layered symmetric structure excited by a prescribed (self-equilibrated) shear edge stress  $P(x_2)$ , an appropriate asymptotic condition becomes

$$\int_0^{h_1} x_2 P(x_2) dx_2 + h_1 \int_{h_1}^{h_1+h_2} P(x_2) dx_2 = 0. \tag{29}$$

This condition ensures the static equilibrium of the soft layer with respect to stress couples applied to both its edge and interfaces; in doing so, the first and second terms in (29) correspond to the contributions of edge  $x_1 = 0$  and interfaces  $x_2 = \pm h_1, x_1 > 0$ , respectively. In fact, this condition is also applicable at leading-order to low-frequency vibration, see [22]. Below, the factor  $e^{-i\omega t}$  is assumed to be omitted. Note that for the frequencies above the cut-off  $\Omega_*$ , this condition becomes a radiation one, prohibiting long-wave propagating modes; see [21].

Let us now implement the substitution

$$P(x_2) = f(x_2) - \sigma_{31}(0, x_2), \tag{30}$$

in (29), where  $\sigma_{31}$  is calculated from (5) starting from the leading-order eigenform (28). This guarantees rapid decay (at the scale of the thickness) of the boundary layer corresponding

to the discrepancy between the given edge load  $f(x_2)$  and the stress  $\sigma_{31}(0, x_2)$  associated with the low-frequency mode of interest. As a result, we arrive at

$$C \approx \frac{1}{ik\mu_2h_1h_2} \left[ \int_0^{h_1} x_2 f(x_2) dx_2 + h_1 \int_{h_1}^{h_1+h_2} f(x_2) dx_2 \right]. \tag{31}$$

The related wave number in the exponential term in (8) is approximated from (24) by

$$k \approx i \frac{1}{h_2} \sqrt{r}, \tag{32}$$

below the cut-off, and

$$k \approx \frac{1}{h_2} \sqrt{r}, \tag{33}$$

above the cut-off, where

$$r = \frac{\mu_1 h_2 - \rho_2 \omega^2 h_1 h_2^2}{\mu_2 h_1}. \tag{34}$$

The last expression satisfies the Sommerfeld radiation principle, also giving room for the simple implementation of the alternative limiting absorption principle; see [23,24] and references therein. To this end, we assume in (34)

$$\mu_j = \mu_{j0}(1 - i\gamma_j), \quad j = 1, 2, \tag{35}$$

where  $\gamma_j \ll 1$ . As a result,

$$r = \frac{h_2(\mu_{10}(1 - i\gamma_1) - \rho_2 \omega^2 h_1 h_2)(1 + i\gamma_2)}{h_1 \mu_{20}(1 + \gamma_2^2)}. \tag{36}$$

It may be seen from the latter that when  $\Omega_2 = \Omega_*$ ,

$$r = - \frac{i\gamma_1 h_2 \mu_{10}(1 + i\gamma_2)}{h_1 \mu_{20}(1 + \gamma_2^2)}. \tag{37}$$

hence, on the cut-off frequency only the absorption over the soft inner layer appears in the expression for  $\text{Im}(r)$ . Clearly, for low-frequency propagating modes (with frequencies above the cut-off) the absorption in both soft and stiff layers needs to be taken into consideration. At the same time, as in most of the cases, the results coming from Sommerfeld and limiting absorption principles agree with each other.

### 6. Conclusions

The developed multiparametric framework for high-contrast elastic laminates demonstrates that degenerated boundary layers do not always coexist with specific low cut-off frequencies. Explicit conditions in the form of strong inequalities on the contrast problem parameters along with numerical illustrations are presented in Section 4.

For a semi-infinite strip, the amplitude of the mode varying slowly both in space and time (decaying or propagating) is determined in Section 5 using a generalisation of Saint-Venant’s principle [19,20] oriented to strongly inhomogeneous laminates. For low-frequency propagating modes, it is shown that the implementation of the limiting absorption principle assumes taking into consideration small dissipation in both the core and skin layers, whereas on the cut-off frequency, only the absorption in the soft inner layer plays a role.

The basic example considered in the paper appears to be highly informative for elucidating a number of important multiscale phenomena characteristic of high-contrast laminates. In particular, it elucidates the general idea of the near-cut-off long-wave be-

haviour typical for elastic waveguides with strong transverse inhomogeneity, characterised by the transition from slowly decaying boundary layers to low-frequency propagating modes. The established framework allows for various extensions, including asymmetric multi-layered thin-walled structures of more general geometry; vector plane and 3D problems; and analysis of various boundary conditions along faces and interfaces, e.g., arising at the mathematical modelling of elastic coatings.

**Author Contributions:** Conceptualization, L.A.A. and J.K.; methodology, J.K. and D.P.; software, L.G.G.; validation, D.P. and L.G.G.; formal analysis, D.P.; writing—original draft preparation, J.K. and D.P.; writing—review and editing, L.A.A. and J.K.; visualization, L.G.G.; funding acquisition, L.A.A. and L.G.G. All authors have read and agreed to the published version of the manuscript.

**Funding:** This research was funded by the Science Committee of Republic of Armenia, within the framework of the research project № 21T-2C075.

**Data Availability Statement:** Data sharing not applicable.

**Conflicts of Interest:** The authors declare no conflict of interest.

## References

1. Aghalovyan, L.A. *Asymptotic Theory of Anisotropic Plates and Shells*; World Scientific: Singapore, 2015.
2. Mikhasev, G.I.; Altenbach, H. *Thin-Walled Laminated Structures*; Springer: New York, NY, USA, 2019.
3. Reddy, J.N. *Mechanics of Laminated Composite Plates and Shells: Theory and Analysis*; CRC Press: Boca Raton, FL, USA, 2003.
4. Liew, K.; Pan, Z.; Zhang, L. An overview of layerwise theories for composite laminates and structures: Development, numerical implementation and application. *Compos. Struct.* **2019**, *216*, 240–259. [[CrossRef](#)]
5. Boutin, C.; Viverge, K. Generalized plate model for highly contrasted laminates. *Eur. J. Mech. A/Solids* **2016**, *55*, 149–166. [[CrossRef](#)]
6. Boutin, C.; Viverge, K.; Hans, S. Dynamics of contrasted stratified elastic and viscoelastic plates-application to laminated glass. *Compos. Part B Eng.* **2021**, *212*, 108551. [[CrossRef](#)]
7. Altenbach, H.; Eremeyev, V.A.; Naumenko, K. On the use of the first order shear deformation plate theory for the analysis of three-layer plates with thin soft core layer. *ZAMM-J. Appl. Math. Mech./Z. Für Angew. Math. Mech.* **2015**, *95*, 1004–1011. [[CrossRef](#)]
8. Aßmus, M.; Nordmann, J.; Naumenko, K.; Altenbach, H. A homogeneous substitute material for the core layer of photovoltaic composite structures. *Compos. Part B Eng.* **2017**, *112*, 353–372. [[CrossRef](#)]
9. Berdichevsky, V.L. An asymptotic theory of sandwich plates. *Int. J. Eng. Sci.* **2010**, *48*, 383–404. [[CrossRef](#)]
10. Boutin, C. High-contrast multi-layered plates. Statics, dynamics and buckling. In *Mechanics of High-Contrast Elastic Solids: Contributions from Euromech Colloquium 626*; Altenbach, H., Prikazchikov, D., Nobili, A., Eds.; Springer International Publishing: Cham, Switzerland, 2023; pp. 39–63.
11. Kuznetsov, S.V. Detection of a hidden sandy layer in a stratified substrate by dispersion analysis. In *Mechanics of High-Contrast Elastic Solids: Contributions from Euromech Colloquium 626*; Altenbach, H., Prikazchikov, D., Nobili, A., Eds.; Springer International Publishing: Cham, Switzerland, 2023; pp. 119–132.
12. Baxter, S.C.; Horgan, C.O. End effects for anti-plane shear deformations of sandwich structures. *J. Elast.* **1995**, *40*, 123–164. [[CrossRef](#)]
13. Wijeyewickrema, A.C.; Horgan, C.O.; Dundurs, J. Further analysis of end effects for plane deformations of sandwich strips. *Int. J. Solids Struct.* **1996**, *33*, 4327–4336. [[CrossRef](#)]
14. Horgan, C. Saint-Venant end effects for sandwich structures. In *Proceedings of the Fourth International Conference on Sandwich Construction*, Stockholm, Sweden, 9–11 June 1998; Volume 1, pp. 191–200.
15. Avila-Pozos, O.; Movchan, A.B. Slow decay of end effects in layered structures with an imperfect interface. *J. Eng. Math.* **2003**, *45*, 155–168. [[CrossRef](#)]
16. Kaplunov, J.; Prikazchikov, D.A.; Prikazchikova, L.A. Dispersion of elastic waves in a strongly inhomogeneous three-layered plate. *Int. J. Solids Struct.* **2017**, *113*, 169–179. [[CrossRef](#)]
17. Ryazantseva, M.Y.; Antonov, F.K. Harmonic running waves in sandwich plates. *Int. J. Eng. Sci.* **2012**, *59*, 184–192. [[CrossRef](#)]
18. Kaplunov, J.; Prikazchikov, D.A.; Sergushova, O. Multi-parametric analysis of the lowest natural frequencies of strongly inhomogeneous elastic rods. *J. Sound Vib.* **2016**, *366*, 264–276. [[CrossRef](#)]
19. Kaplunov, J.; Prikazchikova, L.; Alkinidri, M. Antiplane shear of an asymmetric sandwich plate. *Contin. Mech. Thermodyn.* **2021**, *33*, 1247–1262. [[CrossRef](#)]
20. Prikazchikova, L. Decay conditions for antiplane shear of a high-contrast multi-layered semi-infinite elastic strip. *Symmetry* **2022**, *14*, 1697. [[CrossRef](#)]
21. Babenkova, E.; Kaplunov, J. Radiation conditions for a semi-infinite elastic strip. *Proc. R. Soc. A Math. Phys. Eng. Sci.* **2005**, *461*, 1163–1179. [[CrossRef](#)]
22. Babenkova, E.; Kaplunov, J. Low-frequency decay conditions for a semi-infinite elastic strip. *Proc. R. Soc. A Math. Phys. Eng. Sci.* **2004**, *460*, 2153–2169. [[CrossRef](#)]

23. Nazarov, S.A. The Mandelstam energy radiation conditions and the Umov–Poynting vector in elastic waveguides. *J. Math. Sci.* **2013**, *195*, 676–729. [[CrossRef](#)]
24. Rodnianski, I.; Tao, T. Effective limiting absorption principles, and applications. *Commun. Math. Phys.* **2015**, *333*, 1–95. [[CrossRef](#)]

**Disclaimer/Publisher’s Note:** The statements, opinions and data contained in all publications are solely those of the individual author(s) and contributor(s) and not of MDPI and/or the editor(s). MDPI and/or the editor(s) disclaim responsibility for any injury to people or property resulting from any ideas, methods, instructions or products referred to in the content.